Light-controllable Fano resonance in azo-dye-doped all-dielectric multilayer structure

Motokura, Kengo ; Kang, Byungjun ; Fujii, Minoru ; Nesterenko, Dmitry V. ; Sekkat, Zouheir ; Hayashi, Shinji

(Citation)
Journal of Applied Physics,125(22):223101-223101

(Issue Date)
2019-06-14

(Resource Type)
journal article

(Version)
Version of Record

Journal of Applied Physics

Light-controllable Fano resonance in azo-dye-doped all-dielectric multilayer structure

Cite as: J. Appl. Phys. **125**, 223101 (2019); https://doi.org/10.1063/1.5091820
Submitted: 06 February 2019 . Accepted: 24 May 2019 . Published Online: 11 June 2019

Kengo Motokura, Byungjun Kang, Minoru Fujii, Dmitry V. Nesterenko, Zouheir Sekkat, and Shinji Hayashi

Journal of Applied Physics ARTICLE scitation.org/journal/jap

Light-controllable Fano resonance in azo-dye-doped all-dielectric multilayer structure

Cite as: J. Appl. Phys. **125**, 223101 (2019); doi: 10.1063/1.5091820
Submitted: 6 February 2019 · Accepted: 24 May 2019 ·
Published Online: 11 June 2019

Kengo Motokura,[1] Byungjun Kang,[1] Minoru Fujii,[1] Dmitry V. Nesterenko,[2,3] Zouheir Sekkat,[4,5,6] and Shinji Hayashi[1,4,a)]

AFFILIATIONS

[1]Department of Electrical and Electronic Engineering, Graduate School of Engineering, Kobe University, Kobe 657-8501, Japan
[2]Image Processing Systems Institute of RAS—Branch of the FSRC "Crystallography and Photonics" RAS, Samara 443001, Russia
[3]Faculty of Information Technology, Samara National Research University, Samara 443086, Russia
[4]Optics and Photonics Center, Moroccan Foundation for Science, Innovation and Research (MAScIR), Rabat 10100, Morocco
[5]Faculty of Sciences, Mohammed V University in Rabat, Rabat 10010, Morocco
[6]Graduate School of Engineering, Osaka University, Osaka 585-0871, Japan

[a)]**Electronic mail:** s.hayashi@dragon.kobe-u.ac.jp

ABSTRACT

Active modulation of Fano resonance by light is demonstrated for an all-dielectric multilayer system containing an azo-dye-doped layer. The sample studied consists of a polystyrene layer doped with disperse red 1 (azo dye) molecules, a polyvinyl alcohol layer, and a pure polystyrene layer. In a Kretschmann attenuated-total-reflection configuration, angle-scan reflection spectra of the sample were measured with blue probe light under blue light pumping. The Fano line shape was found to change systematically depending on the intensity of the pump light. Analyses based on electromagnetic calculations of the spectra and field distributions in the layers indicate that the Fano resonance observed is generated by coupling between a broad half-leaky guided mode supported by the azo-dye-doped layer and a sharp planar waveguide mode supported by the pure polystyrene layer. The systematic changes in the Fano line shape under pump light irradiation can be well understood by a systematic decrease in light absorption in the azo-dye-doped polystyrene layer; the decrease in light absorption is due to a decrease in the extinction coefficient of the layer arising from the photoisomerization of azo dye molecules.

I. INTRODUCTION

Over the past decade, great efforts have been made to realize Fano resonances in a variety of plasmonic nanostructures,[1] photonic crystals,[2] and metamaterials,[3] since high-*Q* Fano resonances in these tailored nanostructures have potential applications in optical devices such as switches,[4] sensors,[5,6] and platforms of enhanced spectroscopies.[7–9] The Fano resonance is a resonant phenomenon that exhibits an asymmetric line shape. It was in 1935 that Ugo Fano gave a quantum mechanical explanation of the asymmetric line shapes observed in the absorption spectra of atoms,[10] due to constructive and destructive interferences between a discrete state and a continuum.[11] He derived a simple formula describing the asymmetric line shape. Now, the Fano resonance is known to be omnipresent in a variety of physical systems, not only in quantum systems but also in classical systems.[12,13] Nanostructures made of metals, semiconductors, and dielectrics can support various resonant modes such as surface plasmon modes,[14,15] cavity modes,[16] guided modes,[16,17] and so on. In tailored nanostructures, the Fano resonance is known to emerge, when a broad resonant mode, usually a "bright mode" with a large radiation loss, is managed to couple with a sharp resonant mode, usually a "dark mode" with a small radiation loss.[1–3,12,13]

In recent years, we have pursued studies of the Fano resonance in simple multilayer structures both experimentally and theoretically.[18–27] The samples studied are metal-dielectric-dielectric (MDD) three-layer structures[18–22,25,27] and all-dielectric four-layer (DDDD) structures,[26] which are attached to a high-index prism to construct a Kretschmann attenuated-total-reflection (ATR) configuration. We demonstrated that in angle-scan ATR spectra of these samples, sharp Fano line shapes are generated and can be controlled easily.

Based on the results of electromagnetic (EM) calculations, we clarified the origins of the Fano resonances; in the MDD structure, the resonance originated from the coupling of a broad surface plasmon polariton (SPP) mode propagating at the MD interface with a sharp planar waveguide (PWG) mode supported by the outermost D waveguide layer,[18–22,25,27] while in the DDDD structure, the coupling between a broad PWG mode and a sharp PWG mode is responsible for the generation of the resonance.[26] The *Q*-factor achieved in the DDDD structure is as high as 2800.[26] Results of our numerical analyses suggest that when the MDD structure is applied to the refractive index sensing of the surrounding medium, the figure of merit of the sensitivity can be enhanced by several orders of magnitude relative to that of the conventional surface plasmon resonance sensor.[20] Our multilayer structures are very much suited for developing novel optical devices operated under Fano resonances, because they can be fabricated very easily and high-*Q* Fano resonances can easily be realized in a controlled way.

The Fano resonances in the tailored nanostructures reported so far are passive, i.e., the position and line shape of the resonances are fixed, once the materials and structural parameters are fixed. However, to extend further the applicability of the Fano resonance to optical devices, the development of techniques for active modulation of the resonance is highly required.[28] The modulation of the Fano line shape by applying external perturbations has already been reported in several systems. By integrating single-layer graphene with a high-*Q* Fano-resonant metasurface, Shvets *et al.*[29,30] demonstrated that the mid-IR reflectivity can be modulated by electrostatic gating. Cui *et al.*[31] verified mechanical tuning of Fano resonances in an array of plasmonic heptamers fabricated on a stretchable polydimethylsiloxane membrane. Xu *et al.*[32] established temperature-tunable Fano resonances in a single crystal of TaAs. Tiguntseva *et al.*[33] realized tunable Fano resonances in halide perovskite nanoparticles with the aid of chemical doping. Among others, the active modulation of Fano resonances by light irradiation is thought to be very important to develop active optical devices such as all-optical switches. In our previous studies,[23,24] we have demonstrated light-tunable Fano resonances in a multilayer system. Doping of azo-dye molecules into the outermost D waveguide layer in the MDD multilayer structure allowed us to tune the resonance position by pump light irradiation. In spite of great efforts devoted so far, only a few reports exist on the active Fano resonances, and further experimental and theoretical studies are strongly demanded.

In realizing the light-tunable Fano resonance in our previous studies,[23,24] we used a poly(methyl methacrylate) (PMMA) waveguide layer doped with disperse red 1 (DR1) molecules. DR1 molecules are one of the azobenzene derivatives and strongly absorb light in the blue-green spectral region. They are known to undergo *trans-cis* isomerization under irradiation of pump light in the absorption region (photoisomerization).[34–40] Effects of light irradiation on the optical properties of the DR1-doped PMMA layer have been studied extensively, and the photoisomerization of DR1 molecules is known to cause a decrease in the refractive index of the layer in the red-infrared region[34,35] as well as a decrease in the absorption coefficient in the blue-green region.[35,36] In our work, we probed the change in the Fano resonance using red light under blue light pumping (pump-probe ATR measurements) and succeeded in observing a systematic shift of the resonance position as a function of the pump intensity.[23,24] From analyses based on EM calculations of the ATR spectra, we concluded that the shift of the Fano resonance is caused by the decrease in the refractive index of the DR1-doped PMMA waveguide layer at the wavelength of the probe light (633 nm); the decrease in the refractive index leads to the shift of the sharp PWG mode, finally resulting in the shift of the Fano resonance. The dependence of the photoinduced shift of the resonance on the polarization of the pump light could be very well described by an angular hole burning (AHB) model.[24] It should be noted here that in previous pump-probe ATR experiments, the pump irradiation resulted in the shift of the resonance position, but the shape of the resonance was not affected significantly.

To further exploit the potential of the photofunctional DR1 molecules in realizing the active modulation of Fano resonance by light, we extend our previous work to modulate the line shape by pump light irradiation. In this paper, we present experimental and theoretical results on a new multilayer structure consisting of three D layers (DDD structure), one of which is doped with DR1 molecules. In contrast to the previous work on light tuning in the MDD structure,[23,24] we probe the change in the Fano resonance by blue light under blue light pumping. We deliberately chose the wavelength of the probe light to fall within the absorption band of the DR1 molecule to introduce losses in the waveguide thereby generating a broad waveguide mode. In fact, our strategy for realizing light-controllable Fano resonance is to excite a broad guided mode in the DR1-doped layer and modulate its spectral width and height by controlling the absorption in the DR1-doped layer by pump light; the amount of absorption in the blue region is controllable through photoisomerization processes. Fitting the experimental spectra with a generalized Fano function, we demonstrate that the asymmetry parameter of the Fano line shape changes systematically depending on the pump power density. Furthermore, based on EM calculations, we identify the interacting modes that generate the Fano resonance and clarify the mechanism of active modulation by pump irradiation.

II. EXPERIMENTAL

The structure of the sample used in the present work is schematically shown in Fig. 1(a). The sample is composed of three layers: DR1-doped polystyrene (DR1-PS), polyvinyl alcohol (PVA), and polystyrene (PS) layers. All the layers were fabricated by a spin-coating method. First, a DR1-PS layer was spin coated on a cleaned SF11 substrate; a toluene solution of a mixture of PS (PS/solution = 6 wt. %) and DR1 (DR1/PS = 1.5 wt. %) was spun with a rotation speed of 2800 rpm. Then, to deposit a PVA layer on top of the DR1-PS layer, a water solution of PVA (5 wt. %) was spun with a speed of 2200 rpm. Finally, to deposit a PS layer on top of the PVA layer, a toluene solution of PS (6 wt. %) was spun with a speed of 3200 rpm. To remove the remaining solvent, after each spin-coating of the layers, the sample was baked in air on a hot plate at 130 °C for 10 min. To perform pump-probe ATR measurements in the Kretschmann configuration, the sample prepared was pasted onto the bottom surface of a 60°-prism made of SF11 glass with the aid of index matching fluid. In this configuration, we

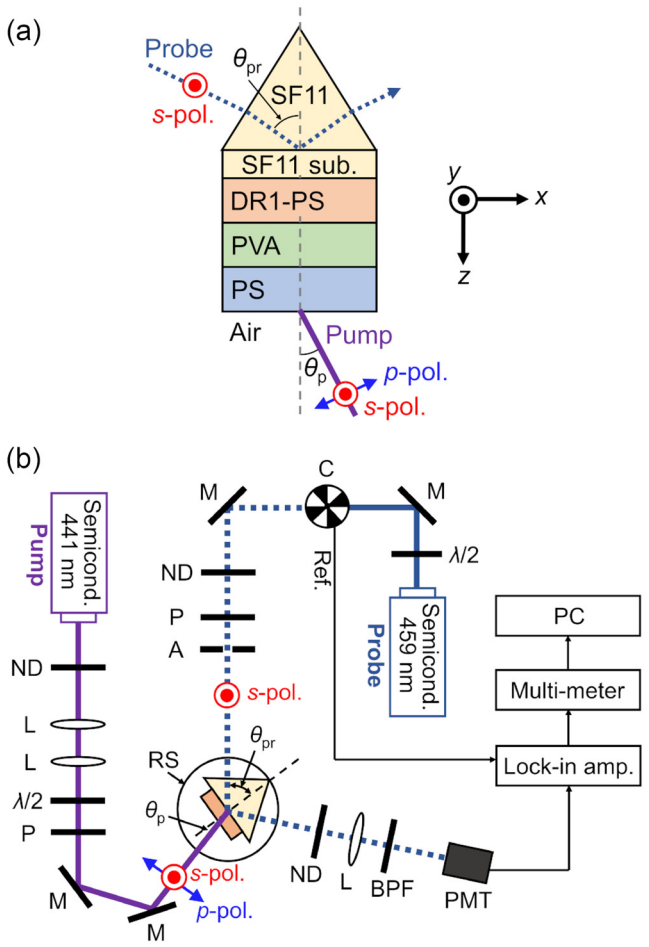

FIG. 1. (a) Multilayer sample consisting of a DR1-doped PS layer, a PVA layer, and a PS layer on a SF11 prism. Kretschmann ATR configuration with pump (441 nm) and probe (459 nm) beams. (b) Pump-probe ATR setup. The *s*-polarized probe beam is used and the polarization of the pump beam is set as *s*-polarization or *p*-polarization. The angle of incidence of the pump beam, θ_p, is ~30°. Optical elements used are half-wave plate ($\lambda/2$), mirror (M), chopper (C), neutral density filter (ND), polarizer (P), aperture (A), rotation stage (RS), lens (L), bandpass filter (BPF), and photomultiplier (PMT).

can regard the SF11 glass substrate, the matching fluid, and the SF11 prism as a single medium.

Figure 1(b) shows an optical setup used for the present pump-probe ATR measurements. The setup is almost the same as that used in our previous work.[23,24] The main difference is the wavelength of the pump and probe beams; instead of using the 488-nm-pump and 633-nm-probe beams, we used the 441-nm-pump and 459-nm-probe beams in the present work. The sample attached to the prism was mounted on a computer-controlled rotating stage. An *s*-polarized light beam from a semiconductor laser with a wavelength of 459 nm (probe beam) was incident on the sample through the prism. To minimize the photoisomerization of DR1 molecules induced by the probe beam, the power density of the probe beam was attenuated by a neutral density filter down to 60 nW/cm^2. The intensity of the totally reflected light exiting from the prism was measured as a function of the angle of incidence with a photomultiplier connected to a lock-in-amplifier. The angle-scan reflectance spectra R were obtained by dividing the intensity data recorded for the sample by those recorded for the bare part of the SF11 prism. To induce the photoisomerization of DR1 molecules, *s*-polarized (parallel polarization) or *p*-polarized (cross polarization) light beam from a semiconductor laser with a wavelength of 441 nm was used as a pump beam. The pump beam was incident on the sample from the air side at an angle of ~30°. The rectangular pump beam ~5 mm in size was adjusted to overlap the circular probe beam ~2 mm in diameter on the sample surface. To cut stray light, in particular that generated by the pump light, a bandpass filter with a maximum transmission wavelength of 460 nm and a full width at half maximum of 10 nm was inserted in front of the photomultiplier.

To obtain a set of data, an ATR measurement without pump irradiation (dark measurement) was first performed, and then the pump-probe ATR measurements were performed under pump irradiation with various pump power densities. The power density was changed from 0.04 to 200 mW/cm^2. After adjusting the power density, the sample was kept under pump irradiation for at least ~1 min to achieve a steady state, and then the ATR measurement was started and completed. The same procedures were repeated in increasing order of the power density. To obtain different sets of data free from possible hysteresis effects of photoisomerization, the measurements were performed on different sample points on the same substrate or different substrates. In addition to the angle-scan ATR measurements, we also performed time transient measurements by monitoring the intensity of the reflected light at a fixed angle of incidence, while switching on and off the pump beam.

III. RESULTS AND DISCUSSION

A. Results of pump-probe ATR measurement

Figures 2(a) and 2(b) show typical data sets of the pump-probe ATR measurements performed under the *s*-pump (parallel polarization) and *p*-pump (cross polarization) conditions, respectively. In the reflection spectra observed under dark, we see a broad dip located at ~59.2° and a sharp asymmetric line shape on the high-angle side of the broad dip around ~59.9°. A close examination of Figs. 2(a) and 2(b) reveals that under pump irradiation, the broad dip becomes shallower and narrower, as the pump power density increases. At the same time, the broad dip shifts systematically to higher angles. Influenced by the changes in the broad dip caused by pump irradiation, the asymmetric resonance is lifted upward, toward higher reflectance values, and its line shape is modified. The position of the steeply decreasing part of the asymmetric resonance fluctuates to some extent but does not show systematic dependence on the pump power density.

In our previous studies on the MDD structure containing a DR1-doped waveguide layer,[23,24] only the shift of the Fano line shape to lower angles was observed as the pump power density increases (light-tunable Fano resonance). Therefore, the behavior of the asymmetric line shape observed in the present work is not the same as that in our previous studies. Comparing Fig. 2(b) with

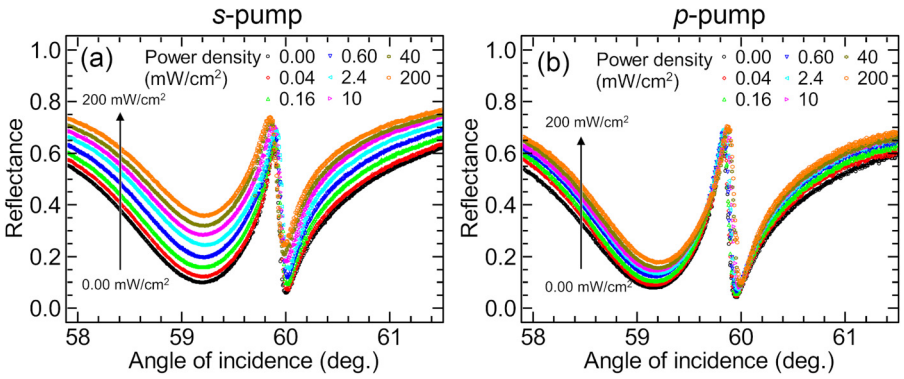

FIG. 2. Results of pump-probe ATR measurement, under parallel polarization (*s*-polarized pump beam and *s*-polarized probe beam) (a) and cross polarization (*p*-polarized pump beam and *s*-polarized probe beam) (b).

Fig. 2(a), we see that the changes in the ATR spectra under cross polarization are much smaller than those under parallel polarization, indicating that the observed phenomena are highly polarization sensitive.

In addition to the angle-scan ATR measurements, we also performed time transient measurements. We fixed the angle of incidence at the reflectance minimum of the broad ATR dip and monitored the intensity of the reflected light, while switching on and off the pump beam. The results of the measurements are given in the supplementary material. As can be seen in Fig. S1 in the supplementary material, the reflectance increases rapidly with a small time constant of ~100 ms, when the pump beam is switched on. On the other hand, when the pump beam is switched off, the reflectance tends to relax very slowly to the initial dark value with a large time constant of ~70 s.

As mentioned before, DR1 molecules undergo reversible *trans-cis* photoisomerization under irradiation of pump light with wavelengths in the blue-green region. *Trans*-DR1 is thermally stable, and it can be considered a rodlike molecule with the largest transition dipole moment along its long axis. *Cis*-DR1 is more globular than *trans*-DR1, and anisotropic optical properties of irradiated DR1-doped polymer films are initiated by photoselection.[40] When irradiated by linearly polarized light, *trans*-DR1 molecules transform into the *cis* form with a probability proportional to $\cos^2\theta$, where θ is the angle between the transition dipole moment and the electric field of the pump light.[34,36] That is, *trans*-DR1 molecules oriented along the polarization direction are selectively photoisomerized, and a hole is burnt into the orientational distribution of the *trans* isomers; this is the basis of the AHB model, which predicts photoinduced anisotropies in DR1-doped polymer films.[34,36,37] *Cis*-DR1 molecules also revert to the *trans* form by photoisomerization or thermal relaxation. After reaching a steady state via multiple isomerization processes, *trans*-DR1 molecules oriented along the direction of pump polarization are depleted. Also, reorientation of DR1 molecules occurs during *trans-cis-trans* cycling, a phenomenon referred to as orientational redistribution (OR). Birefringence and dichroism are direct consequences of the photoisomerization of DR1 molecules under polarized light irradiation, and both AHB and OR as well as rotational diffusion contribute to the observed anisotropy.[34,36,37] Because of the polarization sensitive nature of photoisomerization, the optical responses are much larger for parallel polarization than for cross polarization. As demonstrated in Figs. 2(a) and 2(b), the changes in the ATR spectra presently observed under parallel polarization are much larger than those under cross polarization.

In isomerization processes, thermal relaxation is very slow compared to photoisomerization. Consequently, the transient responses of optical signals in DR1-doped polymer films are very slow when the pump is switched off, whereas it is fast when the pump is switched on. For our sample, we observed this behavior of the time transient (details are present in the supplementary material) and the time constants obtained are in good agreement with those reported for DR1-doped polymer films.[34–37] The strong polarization dependence of the spectral change and the time transient observed in the present experiments allow us to attribute the presently observed light-induced changes in the ATR spectra to the photoisomerization of DR1 molecules in the DR1-PS layer.

B. Fitting with the generalized Fano function

To confirm that the asymmetric line shapes presently observed are Fano line shapes, we attempted to fit the observed spectra with a generalized Fano function derived by Gallinet and Martin.[41–43] Originally, the generalized Fano function was derived to describe Fano resonances in plasmonic nanostructures and metamaterials and is a function of the angular frequency ω. The function was used to fit spectra obtained as a function of photon energy or wavelength. In our ATR geometry, the spectra are measured as a function of the angle of incidence θ_{pr} fixing the wavelength of the incident light. Therefore, it is appropriate to express the function in terms of the in-plane wavevector k_x, which is related to θ_{pr} by $k_x = (2\pi/\lambda)\, n_p \sin\theta_{pr}$, where λ is the wavelength of the probe light and n_p is the refractive index of the prism. As in our previous work,[26] we use the following expression of the generalized Fano function to fit our experimental ATR spectra:

$$\sigma_t(k_x) = \frac{a^2}{\left(\frac{k_x^2 - k_L^2}{2W_L k_L}\right)^2 + 1} \cdot \frac{\left(\frac{k_x^2 - k_F^2}{2W_F k_F} + q\right)^2 + b}{\left(\frac{k_x^2 - k_F^2}{2W_F k_F}\right)^2 + 1}. \quad (1)$$

The first term in the right-hand side is a Lorentzian function representing a symmetric broad resonance and the second term is

an asymmetric function representing the Fano line shape. a^2 is the maximum amplitude of the resonance, k_L is the central position of the resonance, and W_L gives an approximation of the spectral width, for the symmetric resonance. k_F is the central position of the Fano resonance, W_F gives an approximation of the spectral width, q is the asymmetry parameter, and b is the modulation damping parameter, for the Fano asymmetric resonance. Developing an *ab initio* theory of Fano resonances, Gallinet and Martin first derived a function corresponding to the second term of Eq. (1), namely, asymmetric function alone.[41] In actual spectra exhibited by plasmonic nanostructures and metamaterials, an asymmetric line shape is often superposed on a broad symmetric resonance. In these structures, the broad resonance alone can be expressed as the Lorentzian function. To retrieve the characteristic parameters of the respective resonances, the frequency, width, and so on, they combined the Lorentzian function with the original Fano function to establish the generalized Fano function.[42,43] Gallinet and Martin demonstrated that the generalized Fano function reproduces very well the spectra of various systems, such as dolmen nanostructures, oligomers, and photonic crystals.[42,43]

To fit the observed ATR spectra with the generalized Fano function, we converted the angle of incidence of the probe beam θ_{pr} to the in-plane wavevector k_x using the wavelength of the probe light ($\lambda = 459$ nm) and a value of $n_p = 1.8156$, taken from a database.[44] The reflectance R was converted to $1 - R$ as well. In general, for a multilayer system, the energy conservation requires $R + A + T = 1$, where A and T represent the absorptance and transmittance, respectively. In real multilayer samples, this equation is valid when light scattering caused by bulk inhomogeneity in layers and roughness at interfaces is negligibly small, which is the case for our present sample. In the ATR geometry under the total reflection condition, $T = 0$ holds. Therefore, the converted vertical axis $1 - R$ represents the absorptance A. In the following discussion, we present the results of analyses only for the data set measured under parallel polarization, since the light-induced spectral changes are much more significant than those under cross polarization. The solid curves shown in Fig. 3(a) are Fano fit curves for the experimental spectra measured under parallel polarization with the pump power densities of 0.00 (dark), 0.60, and 200 mW/cm^2, respectively; the experimental spectra are the same as those presented in Fig. 2(a). We see that the fit curves reproduce very well the experimental ATR spectra around the asymmetric line shape; we can thus confirm that the presently observed asymmetric line shapes are due to the Fano resonances. The discrepancies between the experimental spectra and the fit curves seen in the high k_x region come from the fact that the broad resonances are not perfectly symmetric exhibiting long tails in the high k_x region. In Figs. 3(b)–3(d), the asymmetric Fano functions, given by the second term of Eq. (1), calculated using the fit parameters are presented for the pump power densities of 0.00 (dark), 0.60, and 200 mW/cm^2, respectively. These figures clearly demonstrate that the Fano line shape can be modified by varying the intensity of the pump light.

The fit parameters obtained for the dark spectrum are $a = 0.986$, $k_L = 2.137 \times 10^{-2}$ nm^{-1}, and $W_L = 2.848 \times 10^{-4}$ nm^{-1} for the symmetric resonance, and $k_F = 2.151 \times 10^{-2}$ nm^{-1}, $W_F = 1.410 \times 10^{-5}$ nm^{-1}, $q = 0.381$, and $b = 0.610$ for the asymmetric resonance, respectively. In Fig. 4, values of the fit parameters obtained for all the spectra

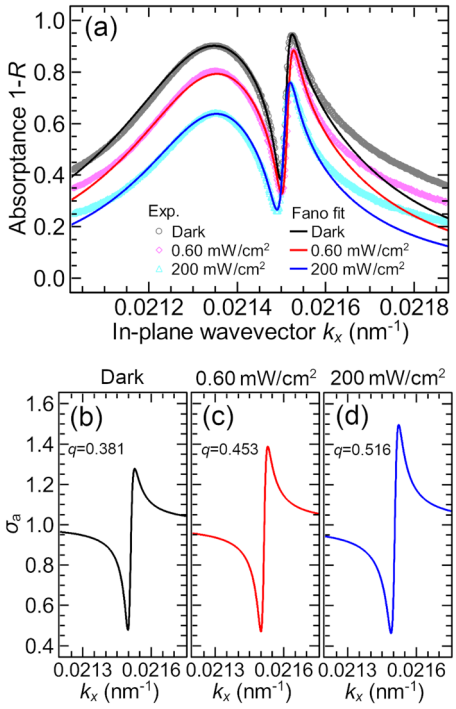

FIG. 3. (a) Experimental spectra (dots) of $1 - R$ under parallel polarization with pump power densities of 0.00 (dark), 0.60, and 200 mW/cm^2, respectively, and corresponding Fano fit curves. Asymmetric Fano functions calculated using fit parameters for 0.00 (dark) (b), 0.60 (c), and 200 mW/cm^2 (d), respectively.

under the pump irradiation are plotted as a function of the pump power density. We see that as the pump power increases, the parameters for the symmetric resonance a and W_L decrease monotonically, while k_L increases slightly, reflecting the systematic shift of the broad ATR dip. For the asymmetric line shape, q increases monotonically from 0.381 to 0.516. Similarly, W_F and b increase monotonically, while k_F fluctuates to some extent but remains almost constant. The decrease in a and W_L reflects the decrease in the amplitude and the broadening of the broad resonance. The slight increase in k_L means that the broad resonance slightly shifts under the pump irradiation. The parameter q is related to the degree of asymmetry of the Fano line shape. Therefore, the change in the value of q gives direct evidence of the change in the Fano line shape. The almost constant k_F means that the Fano resonance does not shift appreciably. These results together with the Fano functions shown in Figs. 3(b)–3(d) clearly demonstrate that the shape of the Fano resonance is controllable by light irradiation without changing appreciably the resonance position.

C. Estimation of optical constants

To estimate the optical constants of the layers in the present sample, namely, refractive index n and extinction coefficient κ, as well as the thicknesses of the layers, we conducted EM calculations of the ATR spectra. The ATR spectra were calculated using a freely

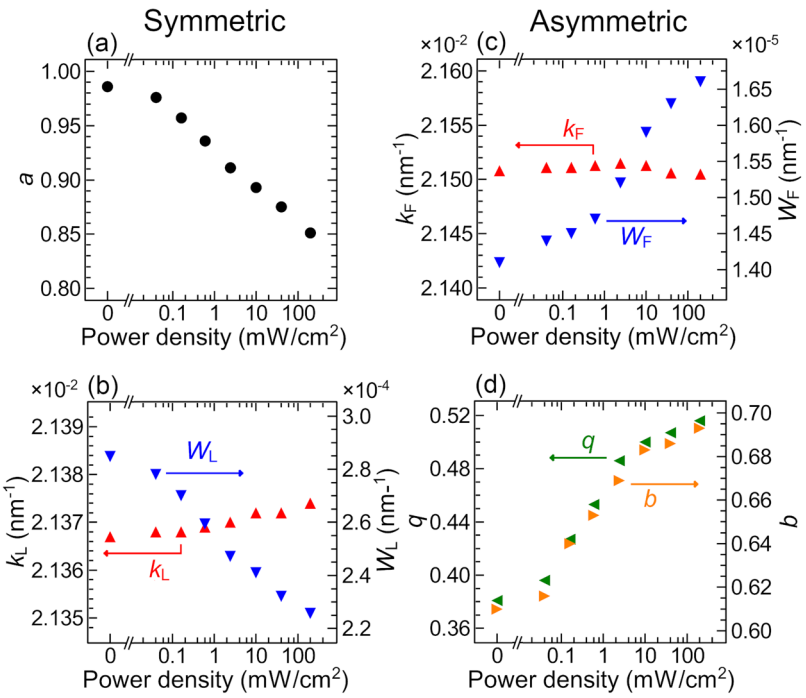

FIG. 4. Dependence of Fano fit parameters on pump power density. (a) a and (b) k_L and W_L, for the symmetric function. (c) k_F and W_F and (d) q and b, for the asymmetric function.

available Winspall software package, which allows us to calculate angle dependent reflectance spectra of multilayer structures based on Fresnel reflection and transmission coefficients.[45] The structural parameters that reproduce well the experimental spectra obtained without and with pump irradiation were searched. The refractive index of SF11 at $\lambda = 459$ nm was set to $n_p = 1.8156$.[44] In Fig. 5(a), the experimental spectra measured under parallel polarization with the power densities of 0.00 (dark), 2.4, and 200 mW/cm^2 [the same spectra as those presented in Fig. 2(a)] are compared with EM fit curves. We see that the EM fit curves reproduce well the experimental ATR spectra. The fit curve for the dark spectrum is generated by a set of parameters: $d_{DR1\text{-}PS} = 423$ nm, $n_{DR1\text{-}PS} = 1.6080$, and $\kappa_{DR1\text{-}PS} = 0.0077$ for the DR1-PS layer; $d_{PVA} = 344$ nm, $n_{PVA} = 1.5256$, and $\kappa_{PVA} = 1.5 \times 10^{-4}$ for the PVA layer; and $d_{PS} = 422$ nm, $n_{PS} = 1.6116$, and $\kappa_{PS} = 1.0 \times 10^{-4}$ for the PS layer. To reproduce the experimental spectra for 2.4 mW/cm^2 and 200 mW/cm^2, the optical constants of the DR1-PS layer were changed from the dark ones to $n_{DR1\text{-}PS} = 1.6083$ and $\kappa_{DR1\text{-}PS} = 0.0049$ for 2.4 mW/cm^2, and $n_{DR1\text{-}PS} = 1.6085$ and $\kappa_{DR1\text{-}PS} = 0.0036$ for 200 mW/cm^2.

In Fig. 5(b), the changes in the optical constants of the DR1-PS layer estimated from the EM fitting, $\Delta n_{DR1\text{-}PS}$ and $\Delta\kappa_{DR1\text{-}PS}$, are plotted as a function of the pump power density. The figure demonstrates that $\Delta\kappa_{DR1\text{-}PS}$ takes negative values falling in the range of 10^{-3} and decreases monotonically, as the pump power increases. We find that the extinction coefficient $\kappa_{DR1\text{-}PS}$ reduces by ~52% relative to the dark value under pumping of 200 mW/cm^2. We note that a much smaller reduction of ~28% is obtained for cross polarization (p-pump). The refractive index increases slightly reflecting the shift of the broad ATR dip; the maximum change is $\sim 0.5 \times 10^{-3}$. The decrease in $\kappa_{DR1\text{-}PS}$ and its polarization dependence are in good agreement with the results of previous studies on the effects of photoisomerization of DR1 molecules on the absorption properties of DR1-doped polymer films.[36,37] Figure 5(b) displays quantitatively the effects of photoisomerization on the optical constants of the present DR1-PS layer.

D. Identification of interacting modes

The Fano resonance is commonly induced by an interference of a broad resonant mode with a sharp resonant mode. To identify the EM modes that generate the Fano resonance in the present sample structure, we performed EM calculations of the ATR spectra for hypothetical multilayer stacks, Stack-1 and Stack-2, schematically shown in the insets of the upper and middle panels of Fig. 6(a), respectively. In Stack-1, the PS layer was removed from the sample structure shown in the lower panel of Fig. 6(a) and a semi-infinite PVA layer was assumed. In Stack-2, only the DR1-PS layer was removed from the sample structure. In the calculations, we used optical constants and thicknesses estimated from the EM fitting of the dark spectrum for parallel polarization. The calculated ATR spectra for Stack-1, Stack-2, and the sample structure are shown in the upper, middle, and lower panels of Fig. 6(a). The spectrum for Stack-1 exhibits a broad dip very similar to that for the sample. The spectrum for Stack-2 exhibits a sharp dip located very close to the position of Fano resonance seen in the spectrum for the sample. The calculated ATR spectra shown in Fig. 6(a) strongly suggest that the Fano resonance in the present sample is caused by the combination between the broad mode supported by Stack-1 and the sharp mode supported by Stack-2.

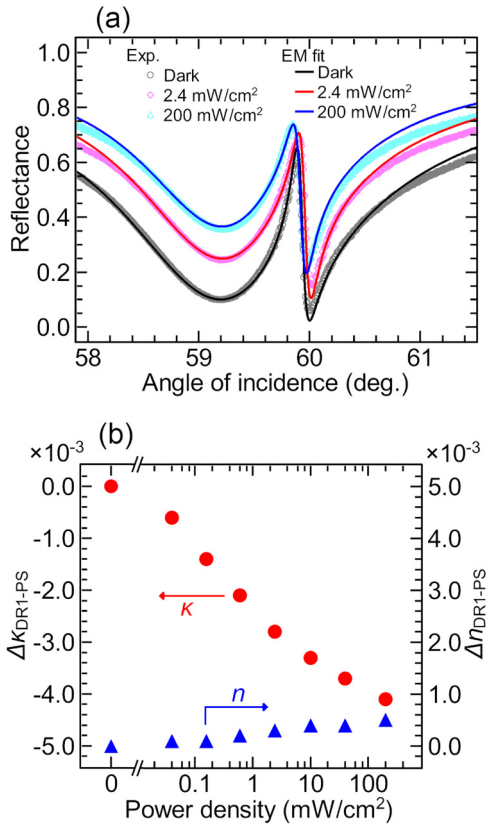

FIG. 5. (a) Experimental ATR spectra (dots) under parallel polarization with pump power densities of 0.00 mW/cm^2 (dark), 2.4 mW/cm^2, and 200 mW/cm^2 and EM fit curves (solid). (b) Changes in optical constants of the DR1-PS layer, $\Delta n_{\text{DR1-PS}}$ and $\Delta\kappa_{\text{DR1-PS}}$, plotted as a function of pump power density.

To gain insight into these modes, we calculated the electric field distributions generated in Stack-1, Stack-2, and the sample structure. In the calculation, we assumed a plane wave incident on the multilayer structure schematically shown in Fig. 1(a). When values of the refractive indices, extinction coefficients, and thicknesses of the layers are known, a transfer-matrix method allows us to calculate the intensities of the reflected and transmitted light as well as the field distributions inside the multilayer structure.[46] The upper, middle, and lower panels of Fig. 6(b) display the field distributions obtained at the angles of incidence corresponding to the minima of the broad dip (59.399°) for Stack-1, sharp dip (59.862°) for Stack-2, and Fano dip (60.001°) for the sample structure, respectively; the positions of the dips are indicated by dots in Fig. 6(a). In Fig. 6(b), the square of the magnitude of the electric field, $|E|^2$, normalized to that of the incident light, $|E_0|^2$, i.e., the electric field enhancement factor, is plotted as a function of the position z in the stack. As shown in Fig. 1(a), z axis is taken normal to the interfaces and the SF11/DR1-PS interface is set at $z = 0$. The field distribution for Stack-1 shows a strong localization of the electric field in the DR1-PS layer. The field inside PVA decays exponentially away from the DR1-PS/PVA interface, while that inside SF11 varies sinusoidally, which is characteristic of a traveling wave. It should be noted that a relation $n_{\text{p}} > n_{\text{DR1-PS}} > n_{\text{PVA}}$ for the present layers leads to these behaviors of the electric fields. In the past, structures similar to Stack-1 have been used frequently to perform optical characterization of liquid crystal layers.[47–49] In these studies, EM modes called half-leaky guided (HLG) modes have been encountered; the EM field associated with the HLG mode decays exponentially away from a waveguide layer on the one hand and exhibits a sinusoidal variation on the other hand. Therefore, the broad mode supported by Stack-1 is identified as a HLG mode.

For Stack-2, we see a strong localization of the electric field in the PS layer; the field decays exponentially on both sides away from the interfaces. This field pattern for Stack-2 is typical of a PWG mode supported by the PS waveguide layer. Therefore, the sharp ATR dip seen in the middle panel of Fig. 6(a) is due to the excitation of a PWG mode. In the present sample structure, the HLG and PWG modes can interact with each other through the overlap of the evanescent fields in the PVA layer. The field distribution of the sample structure shown in the lower panel of Fig. 6(b) clearly demonstrates the hybridized nature of the mode due to the coupling of the HLG and PWG modes. From the ATR spectra and the field distributions presented above, we can finally conclude that the Fano resonance in the present sample is realized by the coupling between the HLG mode supported by the DR1-PS layer and the PWG mode supported by the PS layer.

Compared to the all-dielectric four-layer structure used in our previous work[26] to demonstrate the Fano resonance arising from the coupling of two PWG modes, one layer is missing in the present sample structure; in the present sample, the DR1-PS waveguide layer is directly deposited on the SF11 substrate without inserting a spacer layer [Fig. 1(a)], while in the previous sample, a spacer layer was inserted between the first waveguide layer and the SF11 substrate (see Fig. 1 in Ref. 26). It should be noted that this difference in the sample structure leads to the difference in the broad modes involved in generating the Fano resonance, i.e., a HLG guided mode in the present work and a PWG mode in the previous work. The results presented above clearly demonstrate that the Fano resonance can be generated successfully even when the PWG mode is replaced by the HLG mode. The present three-layer structure is simpler than the previous four-layer structure and thus more advantageous for developing various applications.

E. Mechanism of line shape modulation by light

As demonstrated in Subsection III C, the main effect of pump light irradiation on the present sample is to decrease the extinction coefficient of the DR1-PS layer through the photoisomerization of DR1 molecules. Therefore, it is very much plausible that the decrease in the amount of light absorption inside the DR1-PS layer is the dominant mechanism of the modulation of the Fano line shape. To confirm this mechanism, we calculated the amount of energy absorbed in each layer of the sample. In the present multilayer structure, the electric field distribution similar to that shown in the lower panel of Fig. 6(b) is established and varies depending on the angle of incidence. In this work, the field distribution is expressed in terms of $|E(z)|^2/|E_0|^2$, the field enhancement factor,

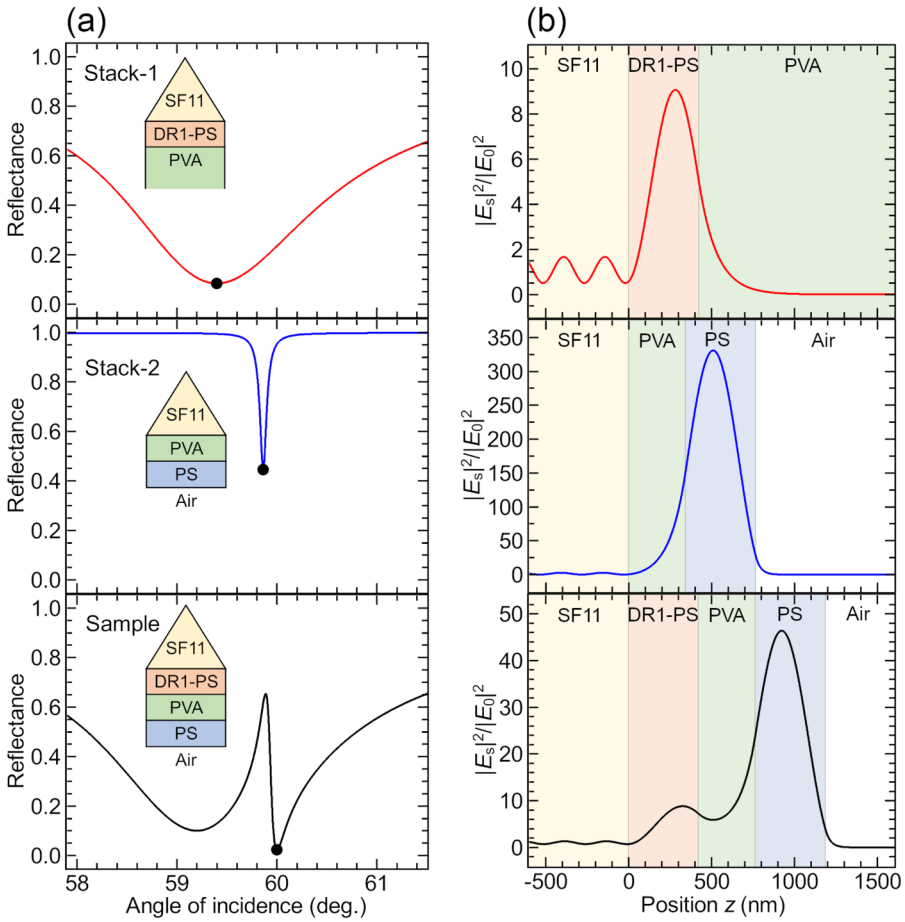

FIG. 6. (a) ATR spectra calculated for Stack-1, Stack-2, and the sample structure, respectively. (b) The electric field distributions calculated for the structures shown in (a). The angles of incidence corresponding to the minima of the dips (dots) seen in (a) were assumed for the calculations.

which depends only on z because of the rotational symmetry of the sample around the z axis [normal to the interfaces, see Fig. 1(a)]. According to the EM theory, the absorption per unit volume around the position $\mathbf{r} = \mathbf{r}_0$ in an absorptive medium is proportional to $\varepsilon_2|\mathbf{E}(\mathbf{r}_0)|^2$, where $\mathbf{E}(\mathbf{r}_0)$ is the electric field at $\mathbf{r} = \mathbf{r}_0$ and ε_2 is the imaginary part of the dielectric constant of the medium given by $\varepsilon_2 = 2n\kappa$.[50] We consider here energy of light incident on unit area at the prism-sample interface and trace a flow of energy in the multilayer. To evaluate the amount of energy absorbed in a layer, we take a volume terminated by unit areas on the interfaces at both sides of the layer. The ratio of the energy absorbed in the volume in the layer to the energy of the incident light per unit area is given by $A(\cos\theta_{pr})^{-1}\cdot\int\varepsilon_2|E(z)|^2/|E_0|^2 dz$, where A is a constant, θ_{pr} is the angle of incidence inside the prism, and the integral is taken over the thickness of the layer. The factor $(\cos\theta_{pr})^{-1}$ accounts for the variation of the incident energy per unit area. Using the above equation together with the electric field distributions, we have calculated the energy absorbed in each layer of the sample as a function of the angle of incidence.

Figures 7(a) and 7(b) show results of the absorption calculation performed for the dark condition and under 200 mW/cm^2 pump irradiation with parallel polarization, respectively. To obtain these results, the optical constants and the thicknesses determined in Subsection III C were used. For simplicity, the constant A is taken to be unity. In the figures, the absorption spectra for three layers and the summation of them (total absorption) are shown. In Fig. 7(a), we see that the absorption in the DR1-PS layer is dominant except for the Fano resonance region. Around the Fano resonance, the absorption in the DR1-PS layer is suppressed and those in the PS and PVA layers exhibit sharp peaks. The broad absorption peak for the DR1-PS layer corresponds to the excitation of the HLG mode. When the angle of incidence approaches the excitation angle of the PWG mode, due to the mode coupling, the electric field inside the DR1-PS layer is strongly suppressed, while a strong electric field is generated in the PS layer, as seen in Fig. 6(b). A strong electric field is also induced in the PVA layer as an evanescent field associated with the PWG mode. Reflecting these behaviors of the electric fields, the absorption in the DR1-PS layer is suppressed and those in the PS and PVA layers exhibit peaks around the Fano resonance.

Figure 7(b) indicates that the absorption in the DR1-PS layer under the pump irradiation is smaller than that under the dark condition by roughly a factor of 2/3 in the whole range. In contrast, the absorption spectra of the PS and PVA layers remain almost the same, exhibiting the peaks. The reduction of the absorption in

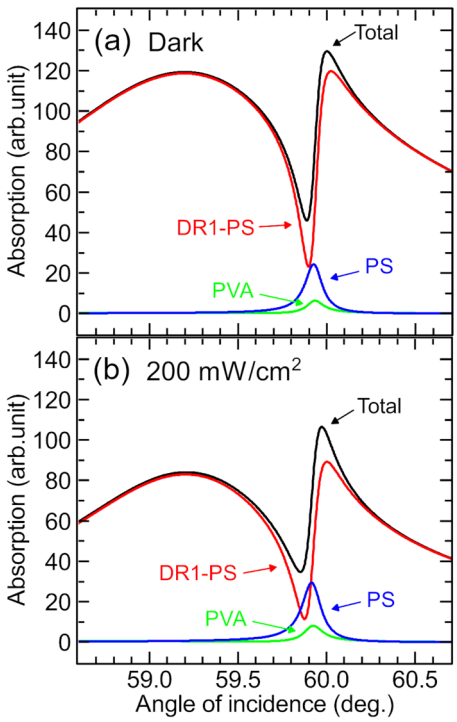

FIG. 7. Absorption spectra of DR1-PS, PVA, and PS layers, and total absorption spectra (summation of all) calculated using parameters for dark (a) and 200 mW/cm^2 (b) pump irradiation in parallel polarization.

the DR1-PS layers is due to the reduction in $\kappa_{\text{DR1-PS}}$ caused by the photoisomerization of the DR1 molecules. From a comparison between Figs. 7(a) and 7(b), we can finally conclude that the change in the Fano line shape presently observed under pump irradiation is caused by the reduction of light absorption inside the DR1-PS layer due to the photoisomerization of DR1 molecules.

We note here that the mechanism of the active modulation of Fano resonance described above is completely different from that reported in our previous papers,[23,24] even though both are based on the photoisomerization of DR1 molecules in the photosensitive layers, i.e., DR1-doped polymer layers. The difference in the mechanism stems from the following two factors. One is the difference in the EM mode modulated by pump light. In fact, in the present DDD multilayer structure, the broad HLG mode supported by the DR1-PS layer is modulated, while in the previous MDD structure, it is the sharp PWG mode supported by the DR1-doped PMMA layer that is modulated. The other factor is the wavelength dependence of the photoinduced change in the optical constants. In principle, when a photosensitive layer is irradiated by pump light, the photoisomerization induces changes in both the refractive index and extinction coefficient. However, the amount of the changes depends on the probe wavelength. The present results shown in Fig. 5(b) demonstrate that when monitored at $\lambda = 459$ nm, the extinction coefficient greatly decreases ($\Delta\kappa_{\text{DR1-PS}} = \sim 4 \times 10^{-3}$) and the refractive index increases slightly ($\Delta n_{\text{DR1-PS}} = \sim 5 \times 10^{-4}$), while at $\lambda = 633$ nm, according to our previous studies,[23,24] the refractive index decreases (typically $\Delta n = \sim 1 \times 10^{-3}$) and no change in the extinction coefficient is detected. These differences lead to different photoresponses of the Fano resonance in the present and previous studies.

For the present sample structure, to recognize correctly the roles played by the photoinduced changes in the refractive index and extinction coefficient of the DR1-PS layer, $\Delta n_{\text{DR1-PS}}$ and $\Delta\kappa_{\text{DR1-PS}}$, we performed EM calculations of the ATR spectra varying independently, $\Delta n_{\text{DR1-PS}}$ and $\Delta\kappa_{\text{DR1-PS}}$, in ranges wider than those achieved experimentally [Fig. 5(b)]. The results are presented in the supplementary material. The calculated results presented in Figs. S2(a) and S2(b) in the supplementary material indicate that the shape of the present Fano resonance is sensitive to $\Delta\kappa_{\text{DR1-PS}}$ and not sensitive to $\Delta n_{\text{DR1-PS}}$. Furthermore, the position of the present Fano resonance is insensitive to both $\Delta\kappa_{\text{DR1-PS}}$ and $\Delta n_{\text{DR1-PS}}$; since the central position of the Fano resonance normally coincides with that of the sharp mode (PWG mode in the present sample),[25,26,42,43] it is not very much affected by the changes in the optical constants governing the broad mode (HLG mode). From these calculated results of ATR spectra, along with those of absorption spectra presented in Figs. 7(a) and 7(b), it is very clear that the present modulation of the Fano resonance is caused by the change in absorption inside the photosensitive layer, which is directly connected to $\Delta\kappa_{\text{DR1-PS}}$.

In our previous studies,[23,24] the Fano resonance shifted without appreciable change in the shape under pump irradiation. This is the direct consequence of the shift of the sharp PWG mode caused by the decrease in the refractive index of the photosensitive waveguide layer at $\lambda = 633$ nm. The structure and the probe wavelength used in the previous studies generated only the shift of the Fano resonance. The experimental and theoretical results presented in this paper and previous papers demonstrate high potentials of DR1 molecules for realizing different types of the active modulation of Fano resonance through photoisomerization processes.

IV. CONCLUSIONS

We have demonstrated light-controllable Fano resonances in ATR spectra of a multilayer structure consisting of a DR1-doped PS waveguide layer, a PVA spacer layer, and a PS waveguide layer. The results of pump-probe ATR measurements clearly demonstrate that the Fano line shape changes systematically depending on the intensity of pump light. The asymmetry parameter of the Fano line shape q determined from the fitting of the experimental spectra to the generalized Fano function increases from 0.381 to 0.516, when the pump power density is increased from 0 to 200 mW/cm^2. We estimated the thicknesses and optical constants of the layers from fitting of the experimental ATR spectra with theoretical spectra calculated by the EM theory. The optical constants obtained for various values of the pump power density suggest that the main effect of the pump light irradiation is to decrease the extinction coefficient of the DR1-PS layer. Since the spectral changes are polarization sensitive and the results of time transient measurements agree well with previous reports, the decrease in the extinction coefficient under pump light irradiation is attributed to the photoisomerization of DR1 molecules in the DR1-PS layer. Based on the results of EM

calculation of the electric field distribution inside the multilayer structure, we concluded that the present Fano resonance is generated by coupling of a broad HLG mode excited in the DR1-PS layer with a sharp PWG mode excited in the PS waveguide layer. Furthermore, the results of EM calculation of the amount of absorption in each layer clearly indicate that the reduction of absorption inside the DR1-PS layer caused by the photoisomerization induces directly the change in the Fano line shape. The present work demonstrates that the photofunctionality of the DR1 molecules (photoisomerization) can be used not only for tuning the Fano resonance as evidenced in our previous work[23,24] but also for controlling the entire Fano line shape. The light-controllable Fano resonance explored here may find potential applications in a variety of optical devices, including switches, sensors, and photonic integrated circuits.

SUPPLEMENTARY MATERIAL

See the supplementary material for the result of time transient measurements, and the response of ATR spectra to changes in optical constants of the DR1-PS layer.

ACKNOWLEDGMENTS

This work was supported by JSPS KAKENHI (Grant Nos. 16K04979 and 16H03828).

REFERENCES

[1]B. Luk'Yanchuk, N. I. Zheludev, S. A. Maier, N. J. Halas, P. Nordlander, H. Giessen, and C. T. Chong, Nat. Mater. **9**, 707 (2010).
[2]M. F. Limonov, M. V. Rybin, A. N. Poddubny, and Y. S. Kivshar, Nat. Photonics **11**, 543 (2017).
[3]A. B. Khanikaev, C. Wu, and G. Shvets, Nanophotonics **2**, 247 (2013).
[4]Y. Yu, M. Heuck, H. Hu, W. Xue, C. Peucheret, Y. Chen, L. K. Oxenløwe, K. Yvind, and J. Mørk, Appl. Phys. Lett. **105**, 061117 (2014).
[5]C. Wu, A. B. Khanikaev, R. Adato, N. Arju, A. A. Yanik, H. Altug, and G. Shvets, Nat. Mater. **11**, 69 (2012).
[6]K.-L. Lee, J.-B. Huang, J.-W. Chang, S.-H. Wu, and P.-K. Wei, Sci. Rep. **5**, 8547 (2015).
[7]S. Yuan, X. Qiu, C. Cui, L. Zhu, Y. Wang, Y. Li, J. Song, Q. Huang, and J. Xia, ACS Nano **11**, 10704 (2017).
[8]K. Thyagarajan, J. Butet, and O. J. F. Martin, Nano Lett. **13**, 1847 (2013).
[9]J. Ye, F. Wen, H. Sobhani, J. B. Lassiter, P. Van Dorpe, P. Nordlander, and N. J. Halas, Nano Lett. **12**, 1660 (2012).
[10]U. Fano, Nuovo Cimento **12**, 154 (1935).
[11]U. Fano, Phys. Rev. **124**, 1866 (1961).
[12]A. E. Miroshnichenko, S. Flach, and Y. S. Kivshar, Rev. Mod. Phys. **82**, 2257 (2010).
[13]E. Kamenetskii, A. Sadreev, and A. Miroshnichenko, *Fano Resonances in Optics and Microwaves* (Springer, New York, 2018).
[14]F. Le, D. W. Brandl, Y. A. Urzhumov, H. Wang, J. Kundu, N. J. Halas, J. Aizpurua, and P. Nordlander, ACS Nano **2**, 707 (2008).
[15]N. Verellen, Y. Sonnefraud, H. Sobhani, F. Hao, V. V. Moshchalkov, P. Van Dorpe, P. Nordlander, and S. A. Maier, Nano Lett. **9**, 1663 (2009).
[16]S. Fan, Appl. Phys. Lett. **80**, 908 (2002).
[17]A. Christ, S. G. Tikhodeev, N. A. Gippius, J. Kuhl, and H. Giessen, Phys. Rev. Lett. **91**, 183901 (2003).
[18]S. Hayashi, D. V. Nesterenko, and Z. Sekkat, Appl. Phys. Express **8**, 022201 (2015).
[19]S. Hayashi, D. V. Nesterenko, and Z. Sekkat, J. Phys. D Appl. Phys. **48**, 325303 (2015).
[20]D. V. Nesterenko, S. Hayashi, and Z. Sekkat, J. Opt. **18**, 065004 (2016).
[21]S. Hayashi, D. V. Nesterenko, A. Rahmouni, and Z. Sekkat, Appl. Phys. Lett. **108**, 051101 (2016).
[22]Z. Sekkat, S. Hayashi, D. V. Nesterenko, A. Rahmouni, S. Refki, H. Ishitobi, Y. Inouye, and S. Kawata, Opt. Express **24**, 20080 (2016).
[23]S. Hayashi, D. V. Nesterenko, A. Rahmouni, and Z. Sekkat, Sci. Rep. **6**, 33144 (2016).
[24]S. Hayashi, D. V. Nesterenko, A. Rahmouni, and Z. Sekkat, Phys. Rev. B **95**, 165402 (2017).
[25]S. Hayashi, Y. Fujiwara, B. Kang, M. Fujii, D. V. Nesterenko, and Z. Sekkat, J. Appl. Phys. **122**, 163103 (2017).
[26]B. Kang, M. Fujii, D. V. Nesterenko, Z. Sekkat, and S. Hayashi, J. Opt. **20**, 125003 (2018).
[27]S. Hayashi, D. V. Nesterenko, and Z. Sekkat, in *Fano Resonances in Optics and Microwaves*, edited by E. Kamenetskii, A. Sadreev, and A. Miroshnichenko (Springer, New York, 2018), Chap. 10.
[28]M. Rahmani, B. Luk'yanchuk, and M. Hong, Laser Photonics Rev. **7**, 329 (2013).
[29]S. H. Mousavi, I. Kholmanov, K. B. Alici, D. Purtseladze, N. Arju, K. Tatar, D. Y. Fozdar, J. W. Suk, Y. Hao, A. B. Khanikaev, R. S. Ruoff, and G. Shvets, Nano Lett. **13**, 1111 (2013).
[30]N. Dabidian, I. Kholmanov, A. B. Khanikaev, K. Tatar, S. Trendafilov, S. H. Mousavi, C. Magnuson, R. S. Ruoff, and G. Shvets, ACS Photonics **2**, 216 (2015).
[31]Y. Cui, J. Zhou, V. A. Tamma, and W. Park, ACS Nano **6**, 2385 (2012).
[32]B. Xu, Y. M. Dai, L. X. Zhao, K. Wang, R. Yang, W. Zhang, J. Y. Liu, H. Xiao, G. F. Chen, S. A. Trugman, J.-X. Zhu, A. J. Taylor, D. A. Yarotski, R. P. Prasankumar, and X. G. Qiu, Nat. Commun. **8**, 14933 (2017).
[33]E. Y. Tiguntseva, D. G. Baranov, A. P. Pushkarev, B. Munkhbat, F. Komissarenko, M. Franckevičius, A. A. Zakhidov, T. Shegai, Y. S. Kivshar, and S. V. Makarov, Nano Lett. **18**, 5522 (2018).
[34]Z. Sekkat and M. Dumont, Appl. Phys. B **53**, 121 (1991).
[35]Z. Sekkat, D. Morichère, M. Dumont, R. Loucif-Saïbi, and J. A. Delaire, J. Appl. Phys. **71**, 1543 (1992).
[36]Z. Sekkat and M. Dumont, Appl. Phys. B **54**, 486 (1992).
[37]Z. Sekkat and M. Dumont, Synth. Met. **54**, 373 (1993).
[38]R. Loucif-Saïbi, K. Nakatani, J. A. Delaire, M. Dumont, and Z. Sekkat, Chem. Mater. **5**, 229 (1993).
[39]Z. Sekkat and W. Knoll, *Photoreactive Organic Thin Films* (Academic Press, San Diego, 2002).
[40]Z. Sekkat, OSA Contin. **1**, 668 (2018).
[41]B. Gallinet and O. J. F. Martin, Phys. Rev. B **83**, 235427 (2011).
[42]B. Gallinet and O. J. F. Martin, ACS Nano **5**, 8999 (2011).
[43]B. Gallinet and O. J. F. Martin, Opt. Express **19**, 22167 (2011).
[44]M. N. Polyanskiy, "Refractive index database," see https://refractiveindex.info (accessed 15 April 2019).
[45]RES-TEC, "Winspall data analysis software," see www.res-tec.de (accessed 15 April 2019).
[46]C. C. Katsidis and D. I. Siapkas, Appl. Opt. **41**, 3978 (2002).
[47]F. Yang and J. R. Sambles, J. Opt. Soc. Am. B **10**, 858 (1993).
[48]N. J. Smith and J. R. Sambles, J. Appl. Phys. **85**, 3984 (1999).
[49]G. Abbate, V. Tkachenko, A. Marino, F. Vita, M. Giocondo, A. Mazzulla, and L. De Stefano, J. Appl. Phys. **101**, 073105 (2007).
[50]L. D. Landau and E. M. Lifshitz, in *Electrodynamics of Continuous Media*, 1st ed. (Pergamon Press, Oxford, 1960), Sec. 61.